Electronic Supplementary information (ESI)

for

Cluster-controlled dimerisation in supramolecular ruthenium photosensitizer-polyoxometalate systems

by

Kirsten Heussner[a,b], Katrin Peuntinger[b], Nils Rockstroh[b], Sven Rau[a]* and Carsten Streb[a]*

[a] Inorganic Chemistry I, School of Chemistry, University of Ulm, Albert-Einstein-Allee 11, 89081 Ulm, Germany, Fax: +49-731-50-23039, Tel: +49-731-50-22575.
[b] Department of Chemistry and Pharmacy, Friedrich-Alexander-University Erlangen-Nuremberg, Egerlandstr. 1, 91058 Erlangen, Germany.

*Email: carsten.streb@chemie.uni-erlangen.de; sven.rau@chemie.uni-erlangen.de

1. Instrumentation

X-ray diffraction: Single-crystal X-ray diffraction studies were performed on a Nonius Kappa CCD Single-crystal X-ray diffractometer or a Bruker APEX II SMART Single-crystal X-ray diffractometer equipped with a graphite monochromator using MoK_α radiation (wavelength $\lambda(MoK_\alpha)$ = 0.71073 Å).

NMR spectroscopy: ^1H- and ^{13}C-NMR spectroscopy was performed on a JEOL EX 400 NMR spectrometer using deuterated solvents as internal standards.

UV-Vis absorption spectroscopy: UV-Vis absorption spectroscopy was performed using a Varian Cary 50 spectrophotometer using a slit width of 2 nm and a scan rate of 480 nm/min. All spectra were recorded using a quartz glass cuvette of 10x10 mm.

FT-IR spectroscopy: FT-IR spectroscopy was performed on a Shimadzu FT-IR-8400S spectrometer. Samples were prepared as KBr pellets. Signals are given as wavenumbers in cm^{-1} using the following abbreviations: vs = very strong, s = strong, m = medium, w = weak and b = broad.

Elemental analysis: Elemental analysis was performed on a Euro Vector Euro EA 3000 Elemental Analyzer.

General remarks: All chemicals were purchased from Sigma Aldrich or ACROS and were of reagent grade. Solvents used were of p.a. grade unless stated otherwise. Chemicals and solvents were used without further purification unless stated otherwise. $[Ru(tbbpy)_2(tmbiH_2)](PF_6)_2$ (**1a**$(PF_6)_2$),[S1] $[Ru(bpy)_2(tmbiH_2)](PF_6)_2$[S1] (**1b**$(PF_6)_2$) and $(TBA)_4[Mo_8O_{26}]$[S2] ($(TBA)_4$**2**, TBA = tetra-*n*-butylammonium) were prepared as described in the literature. Product purity was confirmed using elemental analysis, ^{1}H-NMR-, UV-Vis- and FT-IR spectroscopy.

2. Synthetic section

2.1. Synthesis of compound 3 $[(Ru(tbbpy)_2)_2(tmbi)][Mo_6O_{19}]$ x *ca.* 5 DMF

$[Ru(tbbpy)_2(tmbiH_2)](PF_6)_2$ (51 mg, 41.9 µmol) was dissolved in 10 ml DMF. $TBA_4[Mo_8O_{26}]$ (66 mg, 30.8 µmol)) was dissolved in 10 ml DMF. The two clear solutions were mixed and 2 ml deionized water and 0.5 ml MeOH were added. The reaction mixture was heated to 60 C for 3 days, cooled to room temperature and set up for crystallization by diffusion of ethyl acetate. After a few days, compound **1** was obtained as a dark, microcrystalline product. In order to obtain crystals suitable for single-crystal XRD, the reaction was conducted as described above without heating. Diffusion of ethyl acetate into the reaction mixture gave single crystals of compound **1**. The crystalline product was filtered off, washed twice with ethyl acetate and dried in a desiccator. Yield: 15.2 mg (5.68 µmol, 27.8 % based on Ru). Elemental analysis (dried material) for $C_{90}H_{112}Mo_6N_{12}O_{19}Ru_2$ in wt.-% (calcd.): C 44.38 (44.23); H 5.00 (4.62); N 6.33 (6.88). Characteristic IR bands (in cm^{-1}): 3482 (s), 2972 (s), 1619 (s), 1543 (m), 1482 (m), 1415 (m), 1385 (s), 1254 (w), 1133 (w), 1033 (w), 949 (s), 919 (s), 852 (m), 808 (m), 719 (m), 668 (s).

2.2. Synthesis of compound 4 $[(Ru(bpy)_2)_2(tmbi)][Mo_6O_{19}]$ x *ca.* 4 DMF

$[Ru(bpy)_2(tmbiH_2)](PF_6)_2$ (25 mg, 25.3 µmol) was dissolved in 6 ml DMF. $(TBA)_4[Mo_8O_{26}]$ (32 mg, 15.5 µmol) was dissolved in 4 ml DMF. The two clear solutions were mixed and 0.5 ml deionized water was added. The reaction mixture was stirred at room temperature for 20 h and set up for crystallization by diffusion of ethyl acetate. After *ca*. 3 weeks, single crystals of compound **4** were obtained. The product was filtered off, washed with ethyl acetate and dried under vacuum. Yield: 7.9 mg (3.69 µmol, 16.9 % based on Ru). Elemental analysis (dried material) for $C_{58}H_{48}Mo_6N_{12}O_{19}Ru_2$ in wt.-% (calcd.): C 35.5 (34.9), H 2.48 (2.43), N 8.13 (8.43). Characteristic IR bands (in cm^{-1}): 3425 (m,b), 2899 (m), 1612 (s), 1532 (w), 1453 (m), 1384 (s), 948 (s), 912 (s), 849 (m), 802 (m), 724 (s), 687 (s).

2.3. Synthesis of $(TBA)_4$5: $(TBA)_4[Mo_5O_{15}(PhPO_3)_2]$

The synthesis of the tetra-*n*-butylammonium (TBA) salt of **5** is an adaptation of a reported synthesis which originally gave the ammonium salt.[14] $(NH_4)_6[Mo_7O_{24}]$ x 4 H_2O (10.8 g (8.88 mmol) is dissolved in 60 ml deionized water and an aqueous ammonia solution (25 %, 3.3 ml) is added. To this, phenylphosphonic acid (4.25 g, 26.88 mmol) is added. The solution pH is set to 4.7 using aqueous HCl (6 M). TBABr (15.8 g, 49.0 mmol) is dissolved in 40 ml deionized water. The solution pH is set to 3.1 using aqueous HCl (6 M). Both solutions are mixed and instantly a white precipitate is formed. The pH of the vigorously stirred suspension is set to 4.7 (HCl, 6 M). The precipitate is removed by centrifugation, washed five times with 30 ml portions of deionized water and four times with 30 ml portions of absolute ethanol. The product is dried under vacuum. Yield: 5.33 g (2.48 mmol; 20.3 % based on Mo). Elemental analysis (dried material) for $C_{76}H_{170}Mo_5N_4O_{29}P_2$ in wt.-% (calcd.): C 42.15 (42.54); H 7.71 (7.99); N 2.52 (2.61). Characteristic IR bands (in cm^{-1}): 3470 (s, b), 3055 (m), 2965 (vs), 2876 (vs), 2365 (s), 1653 (m), 1485 (vs), 1437 (m), 1383 (m), 1150 (vs), 1142 (vs), 1123 (vs), 1053 (vs), 984 (vs), 963 (vs), 936 (vs), 924 (vs), 754 (vs), 723 (vs).

2.4. Synthesis of compound 6 $(MeNH_2)_2[(Ru(tbbpy)_2)_2(tmbiH_2)][Mo_5O_{15}(PhPO_3)_2]$ x *ca.* 4 DMF

$(TBA)_4[Mo_5O_{15}(C_6H_5PO_3)_2]$ (20.8 mg, 9.5 µmol) was dissolved in 3 ml DMF. $[Ru(tbbpy)_2(tmbiH_2)]$ (23.4 mg, 19.2 µmol) was dissolved in 3 ml DMF and both solutions were mixed and stirred at rt for 20 h. Single crystals of **6** were obtained by diffusion of diethyl ether into the reaction mixture. After *ca.* 4 weeks, the crystals were filtered off, washed with diethyl ether and dried under vacuum. Yield: 3.7 mg (1.59 mmol, 15.7 % based on Mo). Elemental analysis (dried material) for $C_{82}H_{109}Mo_5N_{14}O_{25}P_2Ru$ in wt.-% (calcd.): C 43.1 (42.21), H 4.79 (4.70), N 8.21 (8.40). Characteristic IR bands (in cm^{-1}): 3358 (m,b), 2969 (m), 1622 (m), 1124 (s), 1095 (s), 954 (s), 908 (s), 862 (m), , 754 (m), 694 (m).

3. Crystallographic section

Single-Crystal Structure Determination: Suitable single crystals of the respective compound were grown and mounted onto the end of a thin glass fiber using Fomblin oil. X-ray diffraction intensity data were measured at 150 K on a Nonius Kappa CCD diffractometer [$\lambda(Mo\text{-}K_\alpha)$ = 0.71073 Å] equipped with a graphite monochromator. Structure solution and refinement was carried out using the SHELX-97 package[S3] *via* WinGX.[S4] Corrections for incident and diffracted beam absorption effects were applied using empirical[S5] or numerical methods.[S6] Structures were solved by a combination of direct methods and difference Fourier syntheses and refined against F^2 by the full-matrix least-squares technique. Diffuse solvent correction was carried out using the SQUEEZE function in Platon.[S7] In compound **6**, the two hydrogen atoms (H102, H104) located on the $tmbiH_2$ nitrogen atoms (N2 and N4) were identified from the difference Fourier synthesis map and constrained using AFIX commands. All other C-H-based hydrogen atoms were added using HFIX/AFIX commands. Crystal data, data collection parameters and refinement statistics are listed in Table 1. These data can be obtained free of charge via www.ccdc.cam.ac.uk/conts/retrieving.html or from the Cambridge Crystallographic Data Center, 12, Union Road, Cambridge CB2 1EZ;

fax:(+44) 1223-336-033; or deposit@ccdc.cam.ac.uk. CCDC reference numbers 823882 (**3**), 823883 (**4**) and 823884 (**6**).

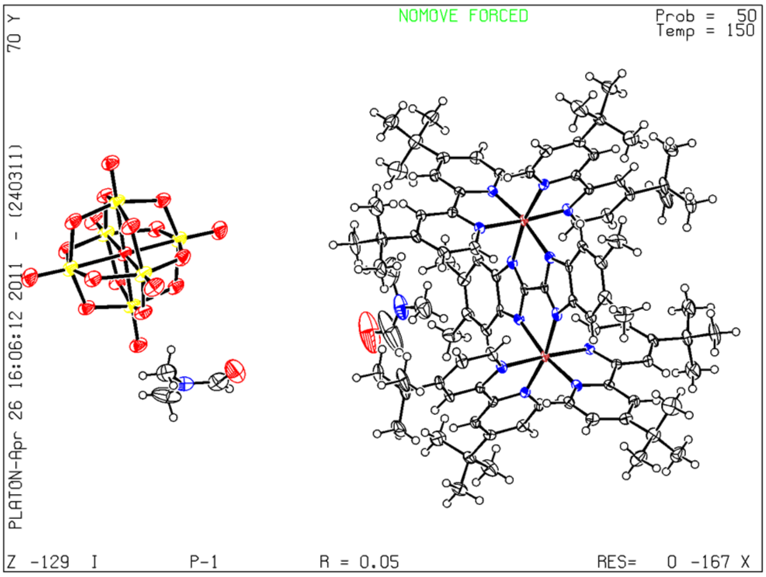

Figure S 1: ORTEP-plot of compound **3**, probability ellipsoids given at 50 %. The anisotropic displacement parameters of the DMF solvent molecules are enlarged due to solvent disorder. All non-hydrogen atoms are refined anisotropically.

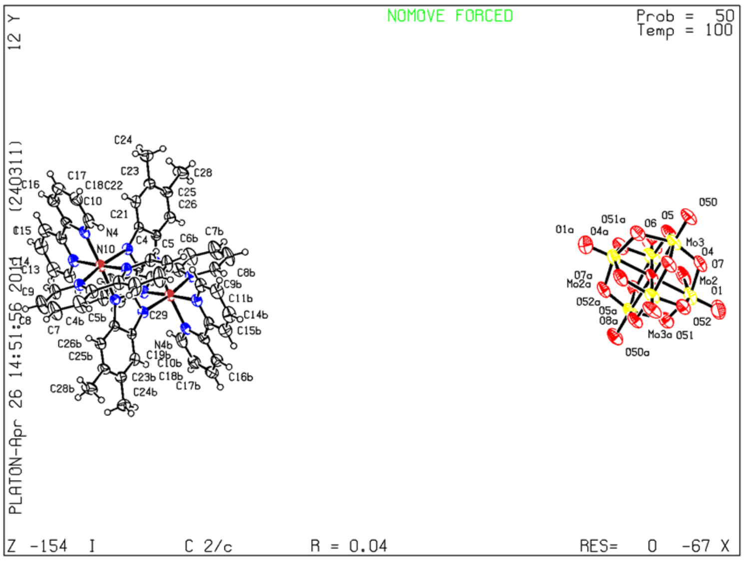

Figure S 2: ORTEP-plot of compound **4**, probability ellipsoids given at 50 %. All non-hydrogen atoms are refined anisotropically.

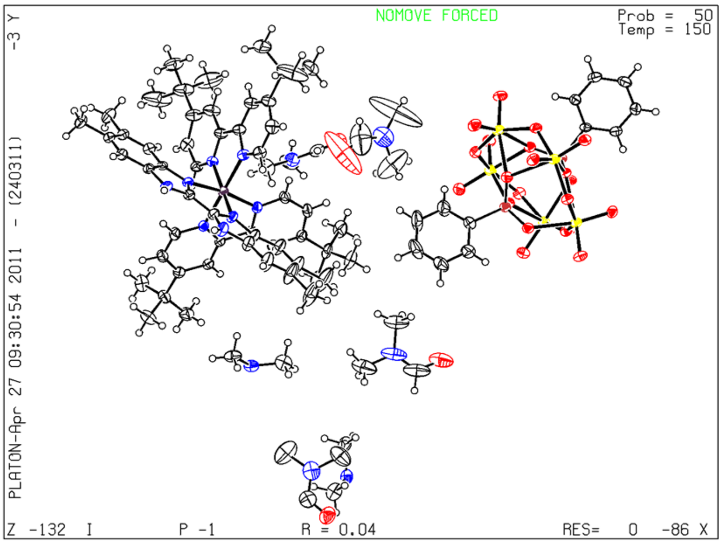

Figure S 3: ORTEP-plot of compound **6**, probability ellipsoids given at 50 %. The anisotropic displacement parameters of the DMF solvent molecules are enlarged due to solvent disorder. All non-hydrogen atoms are refined anisotropically.

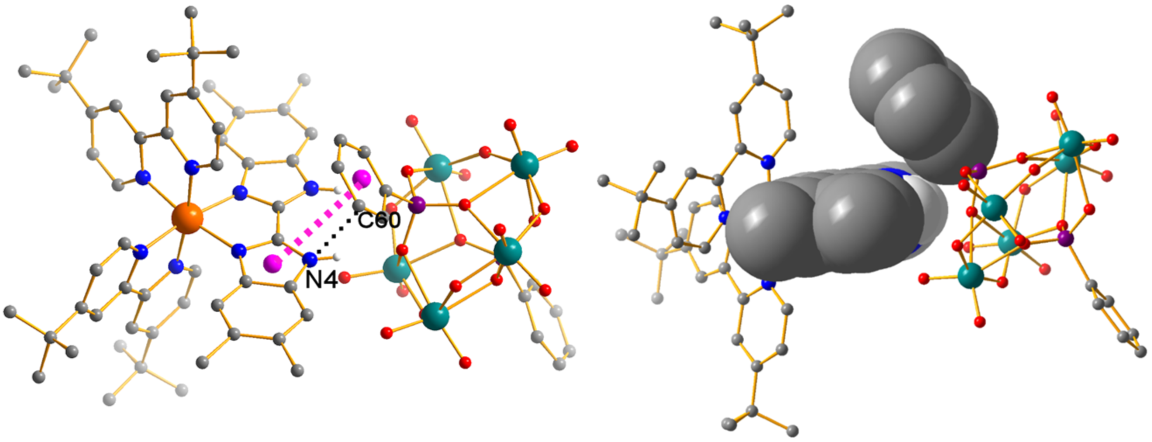

Figure S 4: Representation of the short intermolecular contacts observed between the phenyl rings of the molybdate cluster **5** and the Ru-photosensitizer **1a** in compound **6**. Minimum centroid distance (pink dashed line): 4.428 Å. Minimum overall distance (black dashed line): 3.526 Å (between C60 and N4).

4. ^{1}H-NMR-spectroscopy

4.1. NMR titration experiments

NMR titrations were performed as follows: for each measurement, the Ru-photosensitizer (**1a** or **1b**, respectively) and the molybdate cluster (**2** or **5**, respectively) were weighed out according to the molar ratios required and dissolved in a given volume of DMSO-d_6. The Ru-photosensitizer/molybdate cluster molar ratios were 8:1, 4:1, 2:1, 1:1, 1:2, 1:4 and 1:8.

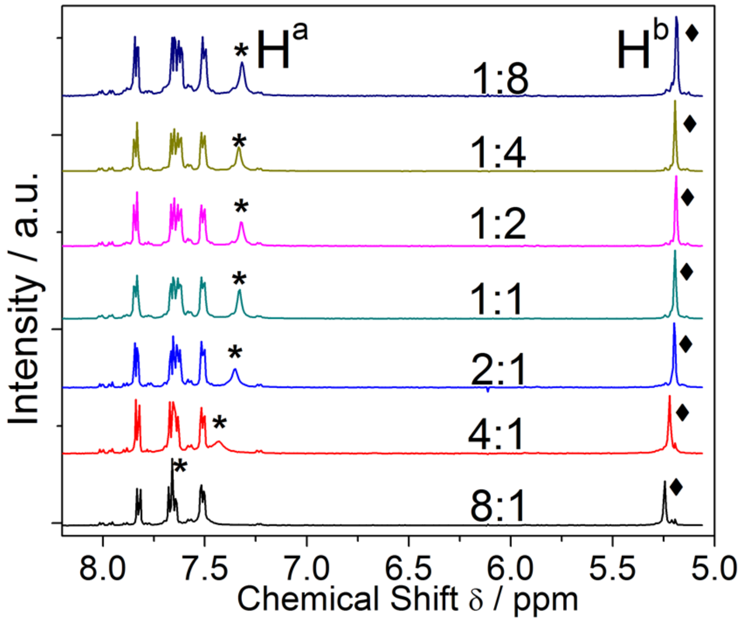

Figure S 5: ^{1}H-NMR spectroscopic monitoring of the changes of the chemical shifts of the tmbiH$_2$-based protons H^a (*) and H^b (♦) depending on the **1a**:**2** molar ratios (1:8 → 8:1).

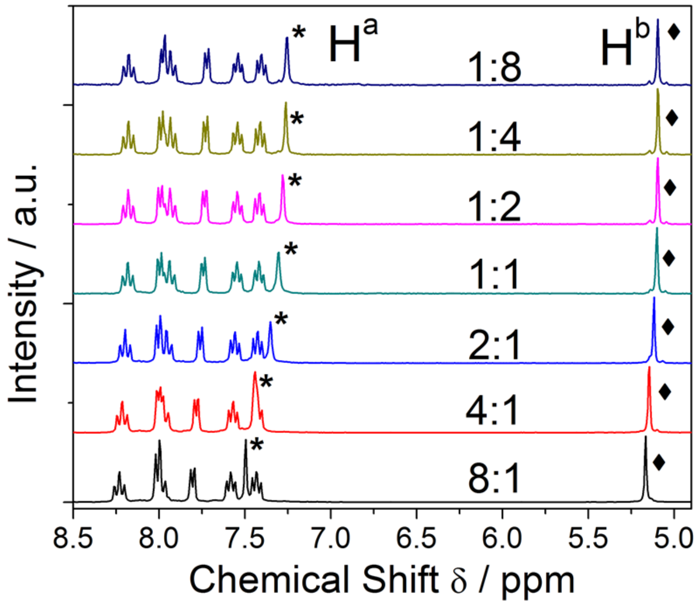

Figure S 6: ^{1}H-NMR spectroscopic monitoring of the changes of the chemical shifts of the tmbiH$_2$-based protons H^a (*) and H^b (♦) depending on the **1b**:**2** molar ratios (1:8 → 8:1).

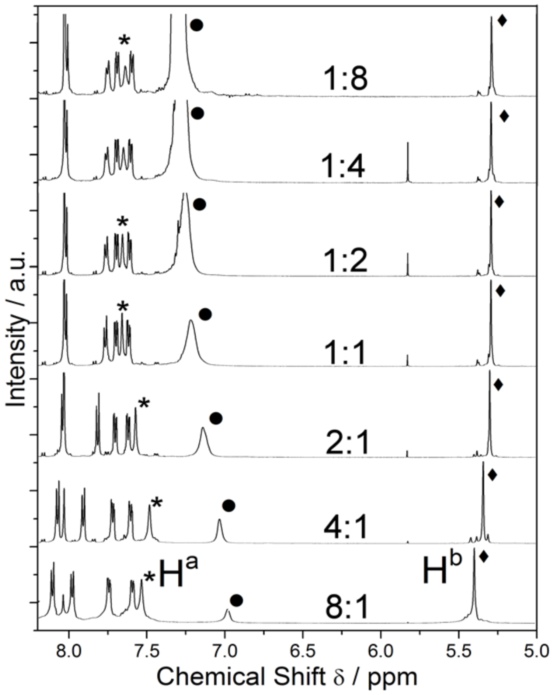

Figure S 7: ^{1}H-NMR spectroscopic monitoring of the changes of the chemical shifts of the tmbiH_2-based protons H^a (*) and H^b (♦) depending on the **1a**:**5** molar ratios (1:8 → 8:1). Additional shifts e.g. of the cluster-based phenyl proton signals (●) can be observed, indicating the presence of further supramolecular interactions, most probably π-π interactions between adjacent aromatic ring systems.

4.2. Time-dependent NMR-measurements

In order to see whether any NMR signals of the formation of the Ru-dimer **3a** are observed, a sample of a typical reaction mixture of **1a** and **2** was prepared using deuterated DMF-d_7 and the sample was monitored over time (30 days). However, no signal change was observed but it was found that an insoluble precipitate had formed after ca. 2 weeks.

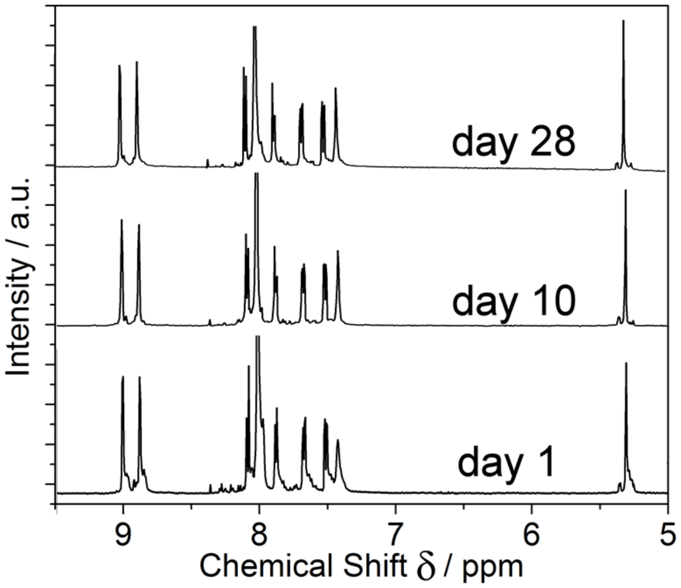

Figure S 8: Time-dependent ^{1}H-NMR spectroscopic monitoring of a reaction solution of the Ru complex **1a** and the molybdate cluster **2** (ratio: 1:1). No changes in the aromatic region of the spectrum were observed, suggesting that the Ru-dimer **3a** is present in solution at very low concentrations only.

5. $[Mo_8O_{26}]^{4-}$ / $[Mo_6O_{19}]^{2-}$ conversion experiments

5.1. UV-Vis spectroscopic measurement of the $[Mo_8O_{26}]^{4-}$ / $[Mo_6O_{19}]^{2-}$ conversion

A 0.98 mM solution of $(TBA)_4[Mo_8O_{26}]$ in DMF was analyzed by UV-Vis spectroscopy at timed intervals. It can be seen that the original spectrum which corresponds to the octamolybdate cluster $[Mo_8O_{26}]^{4-}$ (**2**) (t = 0 h) changes over time to give the UV-Vis spectrum characteristic of the hexamolybdate cluster $[Mo_6O_{19}]^{2-}$ (**3b**) (t = 40 h). An isosbestic point is observed at $\lambda_{isosbestic}$ = 298 nm. The time-dependent increase in $[Mo_6O_{19}]^{2-}$-concentration was monitored at λ = 350 nm, the corresponding cluster concentration was calculated based on the molar extinction coefficient of $[Mo_6O_{19}]^{2-}$: ε_{350} = 5843.2 M^{-1} cm^{-1}.

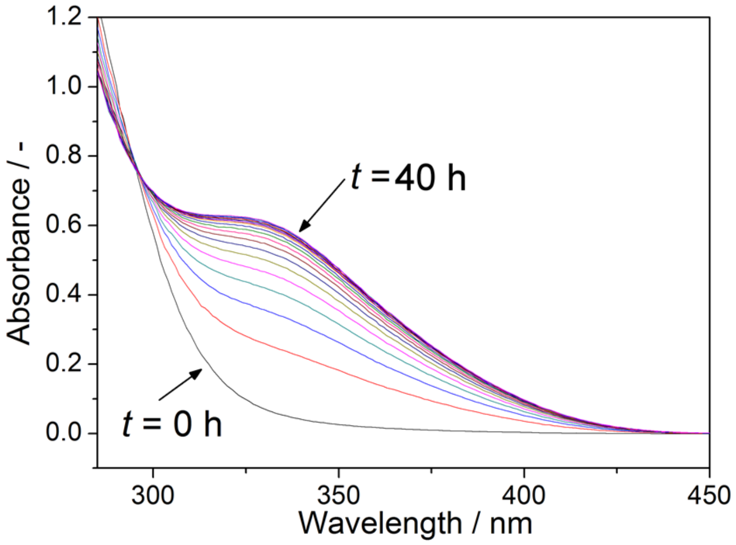

Figure S 9: Time-dependent UV-Vis-spectroscopic measurement of the **2** to **3b** cluster conversion. At *t* = 0 h, the characteristic octamolybdate absorption spectrum is observed. At *t* = 40 h, the characteristic hexamolybdate absorption spectrum is observed.

5.2. pH-measurement of the of the $[Mo_8O_{26}]^{4-}$ / $[Mo_6O_{19}]^{2-}$ conversion

Solutions of $(TBA)_4[Mo_8O_{26}]$ ($[[Mo_8O_{26}]^{4-}$ = 1.0 mM and 4.0 mM, respectively) were prepared in DMF. The solutions were stored in darkness at room temperature to avoid thermal or light-induced reactions. 1 ml aliquots were taken from the solution at timed intervals and hydrolyzed in 5 ml of deionized water. The solution pH was measured (Mettler Toledo FiveGo pH meter). The measurements were repeated twice and the readings were confirmed within the experimental error. The measurements show that the solution pH rises over time, indicating the liberation of hydroxide ions in the aqueous solution. The pH rise shows a similar time-dependency as the $[Mo_8O_{26}]^{4-}$ / $[Mo_6O_{19}]^{2-}$ conversion, see Fig. S9.

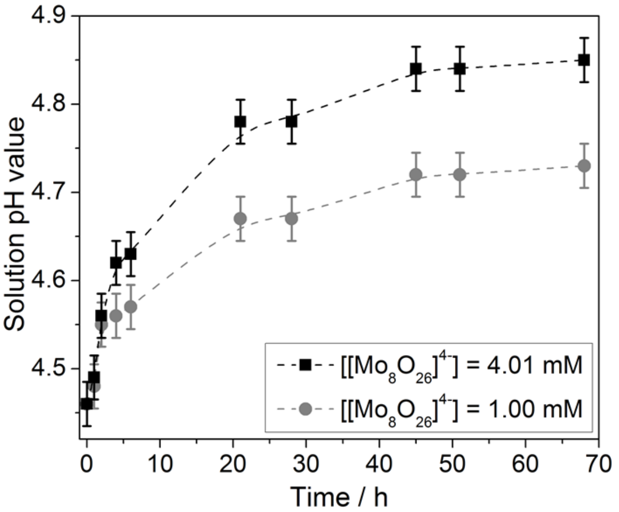

Figure S 10: Time-dependent measurement of the solution pH during the $[Mo_8O_{26}]^{4-}$ / $[Mo_6O_{19}]^{2-}$ conversion**.**

6. Literature references cited in Electronic Supporting Information

S1 S. Rau, B. Schäfer, A. Grüssing, S. Schebesta, K. Lamm, J. Vieth, H. Görls, D. Walther, M. Rudolph, U. W. Grummt and E. Birkner, *Inorg. Chim. Acta*, 2004, 357, 4496.

S2 K. Heussner, K. Peuntinger, N. Rockstroh, L. C. Nye, I. Ivanovic-Burmazovic, S. Rau and C. Streb, *Chem. Commun.*, 2011, DOI: 10.1039/C1CC11859E.

S3 G. M. Sheldrick, *Acta Crystallogr.* 2008, **A64**, 112.

S4 L. J. Farrugia, *J. Appl. Cryst.* 1999, **32**, 837.

S5 R. H. Blessing, *Acta Crystallogr. A* 1995, **51**, 33.

S6 P. Coppens, L. Leiserowitz and D. Rabinovich, *Acta Crystallogr.* 1965, **18**, 1035.

S7 A. L. Spek, *Acta Crystallogr. D* 2009, **65**, 148.